DOI: https://doi.org/10.37434/tpwj2023.12.01

DEVELOPMENT OF PLASMA-ARC TECHNOLOGIES OF SPHERICAL GRANULE PRODUCTION FOR ADDITIVE MANUFACTURING AND GRANULE METALLURGY

V.M. Korzhyk, D.V. Strohonov, O.M. Burlachenko, O.M. Voitenko, D.V. Kunitskyi

E.O. Paton Electric Welding Institute of the NASU
11 Kazymyr Malevych Str., 03150, Kyiv, Ukraine

ABSTRACT

The technological and structural properties of spherical granules and the peculiarities of their production processes using industrial technologies of gas atomization, plasma rotating electrode process and plasma-arc atomization of neutral and current-carrying wires and rods are considered. It was found that among the considered methods of obtaining spherical granules, the most promising in terms of productivity, energy efficiency and simplicity of the equipment used is the method of plasma-arc atomization, which, due to the presence of a large number of technological and structural parameters of the process, allows adjusting the particles size distribution and technological properties of the granules in a wide range. Experimental studies have shown that the particles size distribution, shape factor and technological properties of granules from titanium alloys and stainless steel obtained by plasma-arc atomization of current-carrying wire materials at the E.O. Paton Electric Welding Institute of the NAS of Ukraine, together with LLC R&D PLAZER Center, are at the level of the best foreign analogues. A promising direction of increasing the energy efficiency and productivity of the process of obtaining spherical granules for additive manufacturing and granule metallurgy using the technology of plasma-arc atomization of current-carrying rods with a diameter of more than 50 mm at reverse polarity by plasma trons with a hollow copper anode is proposed.

KEYWORDS: plasma-arc atomization of current-carrying wires and rods, spherical granules, additive manufacturing, selective and direct laser melting and sintering, granule metallurgy

INTRODUCTION

Tendencies in the progress of modern industry in the leading world countries showed that further advances in aerospace, ship-building, power, chemical and biomedical industries are impossible without development and production of new special materials with specified properties and their processing technologies, primarily Additive Manufacturing (AM) [1]. Among the most widely applied AM technologies one should note Bed Deposition technology, which includes the processes of selective and direct laser melting and sintering (Selective Laser Melting (SLM) and Selective Laser Sintering (SLS), DMLS) and Electron Beam Melting (EBM); Direct Energy Deposition technology — a direct energy deposition method, including the processes of laser deposition (Direct Metal Deposition (DMD) and Laser Engineered Net Shaping (LENS) and cold gas-dynamic spraying (Cold Spraying (CS)), and the technology of precision workpiece manufacturing with minimal machining allowance, using the compacting methods of granule metallurgy — Hot Isostatic Pressing (HIP) and oth.

All these methods mainly use specialized spherical granules as the consumable material for forming additive layers and granule composition. These granules should satisfy strict requirements, namely they should have a high degree of sphericity in the absence of satellites and other defects [2, 3], and a certain their size distribution, which for SLM and DMLS processes should be in the range of 15–63 μm, for CS — 15–45 μm, for SLS — 15–80 μm, for EBM — 45–106 μm, for LENS and DMD — 45–150 μm, and for HIP technology — 106–250 μm. Such granules should have minimal porosity and stable chemical and phase composition.

At present, gas atomization is the most widespread technology to produce the granules for additive manufacturing [4]. A certain share in these processes belongs to plasma-arc technologies, featuring a number of advantages [5]. Significant expansion of additive manufacturing application and its transition to a new technological level requires new technologies of producing consumable materials, meeting a number of criteria by their quality, technological characteristics, productivity, cost, etc. In this connection, this work is aimed at solving the following tasks:

- conducting a critical review of the available technologies of producing spherical granules for additive manufacturing and promising directions of their development;
- substantiation of the effectiveness and analysis of new avenues of development of plasma-arc technologies and equipment for producing spherical granules for additive manufacturing and granule metallurgy;

● description of new results in producing spherical granules by plasma-arc atomization of wire materials, as well as rods and large-sized ingots.

REVIEW OF THE AVAILABLE TECHNOLOGIES OF PRODUCING SPHERICAL GRANULES FOR ADDITIVE MANUFACTURING

The main technologies of producing spherical granules for additive manufacturing include: gas atomization (GA) of the melt by inert gas (Free Fall Gas atomization (FFGA), Close-coupled gas atomization (CCGA), Electrode Induction Gas Atomization (EIGA)) and technologies of plasma atomization of wires and rods (Plasma Rotating Electrode Process (PREP) and Plasma Atomization (PA)).

At present GA in the most widely accepted method to produce spherical granules from different metals and alloys for AM. In GA method (Figure 1) the initial material is melted in the shielding atmosphere (vacuum or inert gas) or in air (at open furnace melting).

Then, the produced melt is poured through the atomizer, where the melt flow is fragmented by a flow of high-velocity inert gas (nitrogen, helium, argon), which breaks up the melt into fine drops, which cool down and solidify penetrating inside the atomization chamber, and the dimensions of which can be determined from the following relationship [7]:

$$D_p = \frac{\mathrm{We} \cdot \sigma}{\rho \cdot U^2}, \quad (1)$$

where D_p is the mean particle size, μm; σ is the surface tension force, N/m^2; ρ is the liquid density, kg/m^3; U^2 is the relative velocity between gas and particle, m/s; We is the Weber criterion.

In work [8] it is shown that EIGA atomization at inductor power of 50–70 kW, electrode rotation speed of 15–40 °C/s and atomization pressure of 5–8 MPa allows producing spherical granules from Ti–6Al–4V titanium alloy of 1–400 μm size. Here, the average size of the granules was d_{50} = 145–190 μm, where up to 50 wt.% was made up by granules of 50–180 μm size. It should be also noted that at pressure rise up to 7–8 MPa, the quantity of satellites on individual granules is greatly increased, as a result of individual particles of different size colliding with each other during atomization. Similar results were obtained in [9], where studies of the size distribution of particles from Ti–45Al–2Nb–2Mn titanium alloy, produced by the technology of electric arc melting of the ingot (arc current of 475 A) and further melt atomization at atomization pressure of 5.5 MPa showed that the average granule diameter is d_{50} = 143–168 μm, and less than 35 % of the granules are of < 100 μm size, desirable for AM. The authors [10] note that at inductor power of 240 kW and atomization pressure of 5 MPa at argon flow rate of 18 m^3/min, the productivity of the abovementioned process can be up to 10–75 kg/h for Ti–6Al–4V titanium alloy, and the coefficient of sphericity is not more than 0.83 on average. Here also gas entrapment occurs during granule solidification in GA, which leads to porosity in these granules. Such entrapped pores can greatly increase porosity in parts, made by AM technology, which may reach 0.63 vol.% [11], where even further HIP treatment allows only reducing the pore size and number of pores, but not completely eliminating gas porosity. Thus, despite the high productivity of GA process, the obtained granules are characterized by relatively low coefficient of sphericity, presence of a large number of satellites, and argon-induced porosity, but the particle size distribution of the granules lies in a wide range, where only a small portion is the interval suitable for application in AM.

A wide array of plasma-arc technologies of wire and rod atomization, among which we can highlight PREP and PA methods, belongs to another kind of widely-accepted technologies of producing spherical granules for additive technologies.

During the PREP process the electrode to be atomized is melted by the plasma arc. Under the impact of an off-center force the molten metal spreads radial-

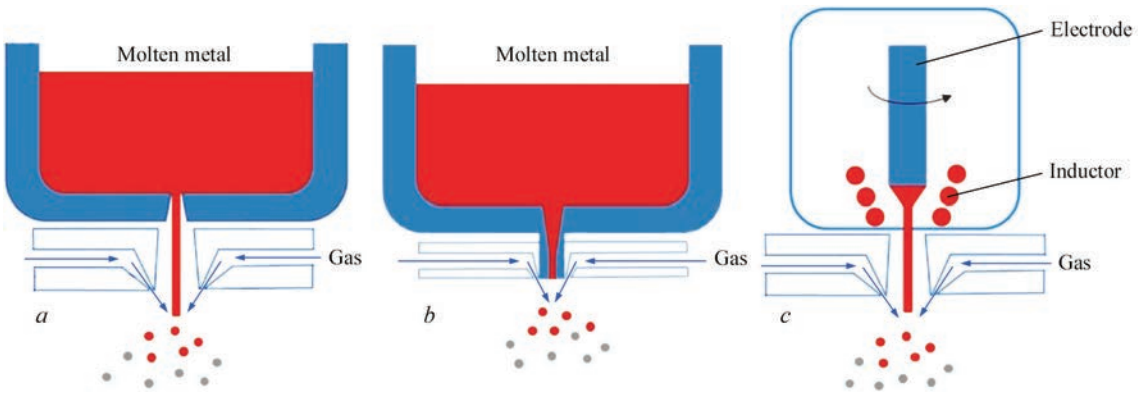

Figure 1. Technological scheme of GA process variants: *a* — FFGA; *b* — FFGA; *c* — EIGA [6]

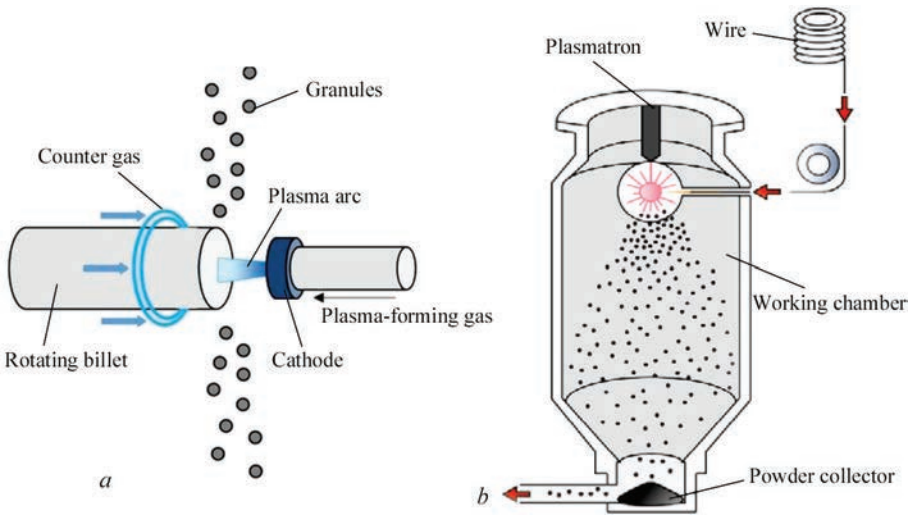

Figure 2. Technological schemes of the processes of plasma-arc atomization of wires and rods: PREP (*a*) and PA (*b*) [16]

ly, forming fine drops, and after that it solidifies into spherical granules, due to the surface tension forces (Figure 2, *a*).

It is known that the billet rotation speed has the greatest influence on the particle size distribution of the granules in the above process [12], where dimensions of atomized granules can be calculated from the following equation:

$$D_p = \frac{K}{\omega} \cdot \sqrt{\frac{\sigma}{\rho \cdot D}}, \qquad (2)$$

where D_p is the mean particle size, μm; σ is the surface tension force, N/m^2; ρ is the liquid density, kg/m^3; ω is the billet rotation speed, rpm; D is the billet diameter, m; K is the correction factor.

In the general case the atomization process is conducted at super high speeds of electrode rotation (up to 9000–25000 rpm), which allows regulation of the particle size distribution in a broad range of 50 to 500 μm. In work [13] it is shown that increase of the billet rotation speed from 9000 to 23000 rpm at PREP atomization of an electrode from Ti–6Al–4V titanium alloy of 55 mm diameter at plasmatron power of 75 kW, allows reducing the average diameter of the granules from d_{50} = 320 to 127 μm. However, there exist considerable difficulties of producing the fine fraction of <75 μm, the proportion of which is not more than 10 wt.%, and which is widely used in additive technology area. That is, the main limitation for PREP is the fact that the available applied rotation speed is not suitable for forming fine granules, which points to a pressing need for designing and producing equipment with a higher speed of electrode rotation. Significant technological difficulties are also encountered in the process of manufacturing the precision billet for atomization, most often using vacuum-induction melting technology, and further machining of the billet. Other drawbacks are impossibility of manufacturing billets from materials of a high hardness and brittleness (Cr–Mo–Fe, Fe–Al, Ni–Al, etc. alloying systems), insufficiently efficient utilization of billet material (stub length is not less than 5 cm on average), low productivity of the process, etc.

A simpler and technologically accessible method of such atomization is plasma atomization of neutral wires and rods of a small diameter, called Plasma Atomization (PA), where melting and dispersion of the material of these wires is caused by the energy and pressure of the plasma jet, generated by three plasmatrons (Figure 2, *b*). It is shown in [14] that the above process can have at least eight adjustable technological and structural parameters of the process, which allow regulation of the particles size distribution of the granules. Here, the granule size can be calculated, using the following equation:

$$D_p = \frac{3.35 \cdot d_n^2}{Q\left(1 + 0.00367 \cdot T\right)} \cdot \sqrt{\frac{d_{dw} \cdot \sigma}{\rho}}, \qquad (3)$$

where Q is the flow rate of plasma-forming gas, m^3/s; d is the plasmatron nozzle diameter, m; T is the mass average temperature of the plasma jet at the nozzle edge, K; d_w is the wire diameter, mm; ρ is the liquid density, kg/m^3; σ is the surface tension force, N/m.

For instance, by changing the plasma-forming gas supply volume, it is possible to change the kinetic energy of the plasma jet, leading to greater or smaller refinement of the melt drops, while change of current supplied to the plasmatron, allows adjustment of the atomized electrode melting rate and volume of the liquid forming at its edge, etc. It should be also taken into account that increase of the atomized electrode diameter, on the one hand, leads to increase of the process productivity, and on the other hand, to lowering of the amount of fine granule fraction of < 80

μm, as at application of large-diameter wires and rods the mass of the melt coming to the atomization zone is increased, and intensity of fragmentation of the initial drops is decreased. Researchers [15, 16] showed that application of a system of three plasmatrons of the total power of 83 kW and plasma-forming gas flow rate of 18–22 m^3/h, allows producing spherical granules from 1.6 mm Ti Grade 2 titanium wire in a rather broad range of 10–300 μm, with average diameter of d_{50} = 189 μm, where O_2 oxygen content is below 0.055 %. The granules are characterized by a minimal number of defective particles, which is not more than 1 wt.% in both the cases, and their porosity is not more than 0.08 vol.%. It should be noted, however, that the maximal productivity of the process for titanium alloys is not more than 1.5 kg/h is the general case.

Critical analysis of the structural, technological and technical-economic characteristics of spherical granules and available technologies of their manufacture showed the following. Presence of a large number of satellites and irregularly-shaped particles, lower coefficient of sphericity for GA technology leads to a difference in some technological characteristics of the granules, compared to PA and PREP. The abovementioned defects create the conditions under which the GA granules "cling" to each other at their mutual displacement (powder feed), which greatly worsens the fluidity values (particularly for the fine fraction of <63 μm), and leads to defect formation in the deposited layers. Intragranular argon-induced porosity for GA granules is impossible to remove by HIP in some cases. In other cases at further heat treatment of the parts the gas opens up the regions in which it is trapped as a result of material heating in the single-phase area, and porosity with ~0.1 % volume fraction forms. Pore opening leads to significant lowering of the values of ultimate strength, impact toughness and other mechanical characteristics of the parts, which are formed by layer-by-layer deposition. Such a microstructural defect is inadmissible for such critical parts as turbine discs, nozzle path parts, etc. Here, the PREP and PA technologies are characterized by a practically complete absence of gas porosity in the granules. PREP and PA methods also feature granule crystallization at super high cooling rates, creating the conditions for formation of a microcrystalline (and in some cases nanocrystalline) structure, which has a positive effect on the mechanical properties of the products made from them. Also important is the fact that for GA process the gas-to-metal ratio (GMR) [17] (flow rate of atomizing gas (argon) required to produce 1 kg of powder) can be from 26 to 110, and for PA and GA processes it is not higher than 8 (for Ti–6Al–4V). PREP equipment operation runs into considerable difficulties related to producing a fine fraction of <100 μm. To achieve more than 50 wt.% yield of the abovementioned fraction, it is necessary to significantly increase the billet rotation speed (more than 30000 rpm), which even more complicates the already not at all simple kinematic diagram of the unit (for lowering the vibration level, designing complex bearing systems, etc). We can also include here the difficulties, associated with producing a cylindrical billet of precise dimensions, which has to be polished with a high precision. At present, the scopes of producing the spherical granules by PA technology do not satisfy the needs of additive manufacturing of products, because of its low productivity, leading to overpriced powders, as well as delays in delivery times. Therefore, it is rational to consider this process now only for use under laboratory conditions, when manufacturing small test batches of powder.

This leads to the conclusion that the technology of plasma atomization has a significant potential for further development and practical application in spherical granule manufacturing. One of its variants is the process of plasma-arc atomization of current-carrying wire materials [14]. The above process is characterized by a higher productivity level [18], which can be up to 12–16 kg/h, and simplicity and mobility of the equipment, which allows application of a wide range of standard consumable materials from solid and flux-cored wires and rods; a large number of technological and structural parameters, permitting regulation of the particle size distribution in a broad range of 15–315 μm. Here, the amount of <100 μm fraction can be up to 90 wt.%.

PWI DEVELOPMENTS IN THE FIELD OF PLASMA-ARC TECHNOLOGIES OF PRODUCING SPHERICAL GRANULES FOR ADDITIVE TECHNOLOGIES. NEW DIRECTIONS IN TECHNOLOGY AND EQUIPMENT DEVELOPMENT

In order to increase the efficiency of the processes of manufacturing spherical granules with the specified particle size distribution and sphericity parameters, at PWI they are currently being developed in two main areas of technology and equipment for:

- plasma-arc atomization of wire materials of 0.8–3.5 mm diameter (solid and composite, for instance with a metal sheath and powder core);
- plasma-arc atomization of rods and ingots of up to 50 mm and larger diameter.

The main technological variants for implementation of the first group of technologies are shown in Figure 3, *a, b*. Here melting of the current-carrying

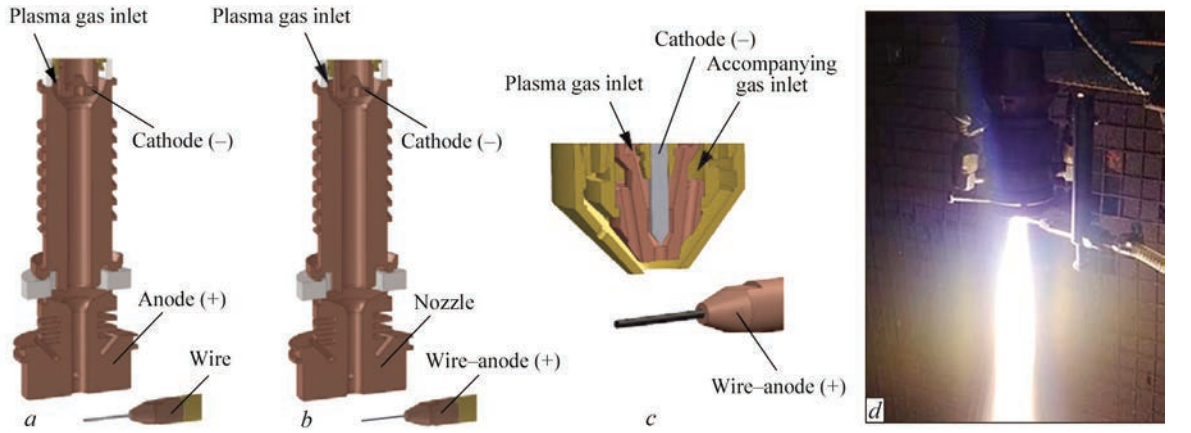

Figure 3. Scheme of the process of plasma-arc atomization of neutral wire (*a*), current-carrying wire without accompanying flow (*b*), current-carrying wire with accompanying gas flow (*c*) and appearance of the atomization process (*d*)

wire-anode, fed into the zone of high-velocity plasma jet, and further dispersion of the melt from the wire edge, are performed. The arc runs between the non-consumable tungsten cathode and current-carrying wire-anode, fed behind the plasmatron nozzle edge, and in the case of neutral wire atomization — between the cathode and plasmatron anode. The working (plasma-forming) gas coming to the working chamber is heated by the electric arc and flows out of the nozzle in the form of a plasma jet.

Results of analysis of energy efficiency and productivity of the processes of plasma-arc atomization of the neutral and current-carrying wires, in the case of atomization of titanium wire of Ti Grade2 at plasma arc power of 15 kW confirmed [19] that atomization of current-carrying wire allows increasing the wire heating efficiency more than 4 times (η = 17 and 4 %, respectively) relative to the method of neutral wire atomization, which in its turn allows increasing the process productivity from 1.5 to 12 kg/h (for titanium wire of Ti Grade2), and energy efficiency up to 6 times. However, despite the relatively low productivity, the method of neutral wire atomization is still widely used in PA technology to produce high-quality commercial spherical powders from reactive, refractory and other high-alloyed metals and alloys (AP&C, Pyrogenesis, Canada [20]).

Note that the method of plasma-arc atomization of current-carrying wire without accompanying gas application can provide a high productivity of the atomization process, which at 20–25 kW power can be equal to 10–12 kg/h for tungsten wire. However, a significant disadvantage of the above process is a wide size distribution of the atomized particles in the range of 40 to 1000 μm [21].

A further development of this process was designing and producing serial UN-126 and KT-088 (PWI) [22] and PLAZER 30-PL-W units (Scientific & Production Center PLAZER, Ukraine) [23], where the abovementioned disadvantages was eliminated by application of an accompanying gas flow (Figure 3, *c*). The accompanying gas flow, directed coaxially to the plasma one, forms the configuration of the latter, promotes its compression and thus reduces the angle of opening of the atomized particle plume, increases the outflow velocity and dynamic pressure of the plasma jet, which in its turn creates the conditions for producing the optimal particle size distribution and chemical composition of the dispersed phase. The data obtained by the results of mathematical modeling [24], showed (Figure 4) that the submerged jet flowing into the atmosphere, rather quickly expands, while mixing intensively with the external gas atmosphere. Plasma jet blowing by a circular laminar flow of cold gas of

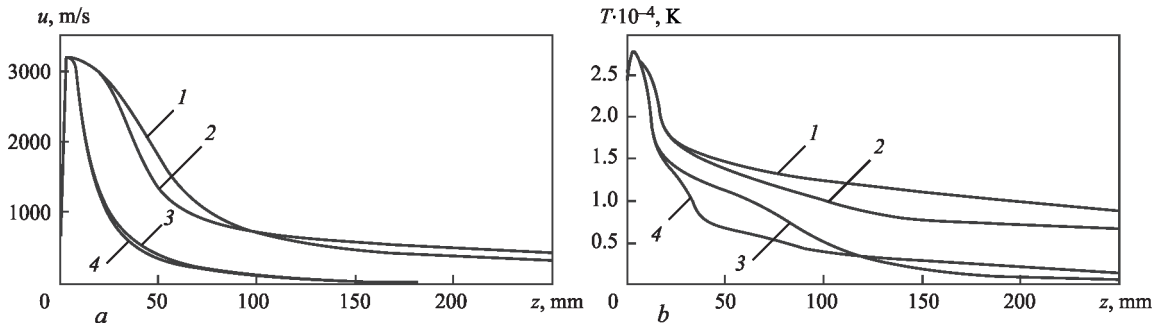

Figure 4. Longitudinal changes of velocity *u* (*a*) and temperature *T* (*b*) of argon plasma flowing out into argon (*1*, *3*) and air (*2*, *4*) atmosphere in different modes of plasmatron operation (current *I* = 200 A), plasma-forming gas flow rate Q_{pl} = 2 m³/h): *1*, *2* — accompanying gas flow rate Q_{ac} = 20 m³/h for argon and air, respectively; *3*, *4* — Q_{ac} = 0 m³/h [24]

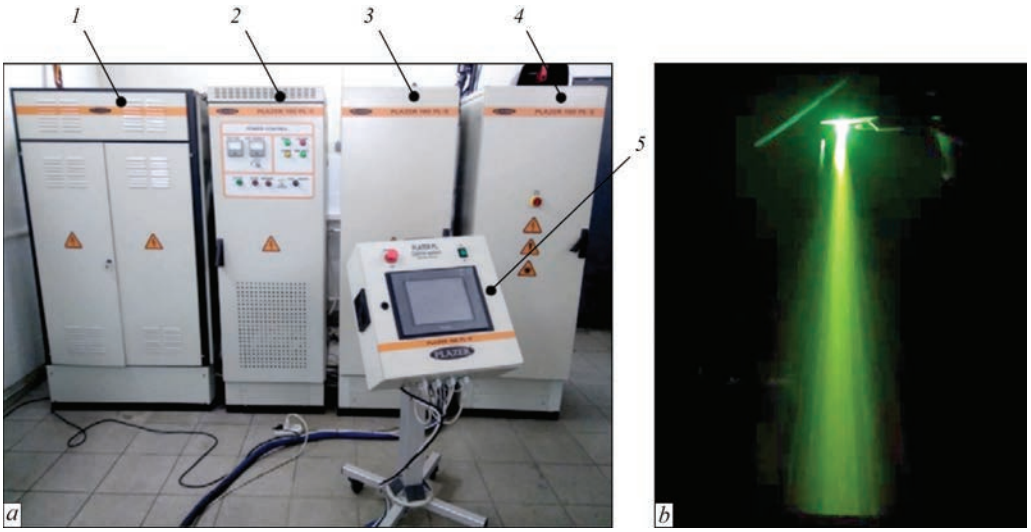

Figure 5. Appearance of PLAZER 50-PL-W laboratory unit (*a*) and two-phase plasma jet (*b*): *1* — transformer power source of the main arc; *2* — thyristor electric drive; *3* — transformer power source of pilot arc; *4* — control and gas preparation cabinet; *5* — mobile operator console with touch panel

the same composition as the plasma-forming one prevents the plasma jet expansion. Here, the turbulence is partially damped by the surrounding circular flow, and the jet energy and pulse are preserved at greater distances than for the submerged jet.

Increase of the velocity of plasma jet outflow in the zone of wire location promotes an increase of gas-dynamic pressure of the jet on the wire edge and transition from vibrational breakup, We = 8–12, and bag breakup, 12 < We < 50, to the mechanism of bag-and-stamen breakup, 50 < We > 100. Here, the intensity of breakup of the melt drops forming at the current-carrying wire edge at its melting, is significantly increased [25]:

$$\mathrm{We} = \frac{\rho_g \cdot u_{rel}^2 \cdot d_p}{\sigma}, \qquad (4)$$

where ρ_g is the gas phase density, kg/m^3; u^2_{rel} is the relative speed between the gas phase and the particle, m/s; d_p is the particle diameter, m; σ is the force of the drop surface tension, N/m.

Experimental data [14] showed that use of accompanying gas flow allows significant reduction of maximal drop dimensions from d_{90} = 1000 to 315 μm, which enables an essential increase of the amount of the fraction suitable for use in AM and granule metallurgy technologies.

Over the recent years development of this technology of plasma-arc atomization consisted in solving tasks related mainly to extension of service life of plasmatron internal parts, improvement of productivity and efficiency of heating and of atomization material utilization. For this purpose, the Scientific & Production Center PLAZER, Ltd. designed and manufactured an experimental-production unit PLA-

Table 1. PLAZER-50-PL-W unit specification

Parameter	Value
Consumed power, kW, not more than	50
Voltage of 50 Hz three-phase AC mains, V	380
Open-circuit voltage, V	160
Range of working current adjustment, A	100–500
Range of working voltage adjustment, V	30–100
Duty cycle, %	100
Air flow rate at 0.6 MPa pressure, nm^3/h	15–60
Argon or helium flow rate at 0.1 MPa pressure, nm^3/h	1–3
Wire feed rate, m/min	2–15
Plasmatron cooling	Air or water
Service life of plasmatron nozzle and cathode, h (machine time)	Not less than 100
Cooling water pressure, MPa	0.3–0.5
Cooling water flow rate, nm^3/h	0.4–0.6
Diameters of applied wire materials, mm	1.0–2.4
Control type	Automated
Controller type	PLC

ZER 50-PL-W (Figure 5), which incorporated a new design of the plasmatron with water cooling and optimized geometry of the nozzle part of reduced overall dimensions, which allowed the abovementioned equipment power to be increased from 30 to 50 kW (Table 1) [18].

This, in its turn, allowed increasing the process productivity to 16–18 kg/h, and intensifying the processes of dispersion of the melt forming at the wire edge. It should be also noted that power increase becomes particularly relevant for the case of flux-cored wire atomization, where increase of flux-cored wire diameter from 1.6 to 2.4 mm and more allows greatly increasing the wire FF (up to 40 %) and, the degree of granule alloying, respectively, but requires ensuring a proper degree of metallurgical interaction of the components, present in the flux-cored wire composition, which leads to lowering of the degree of granule heterogeneity by their chemical and phase composition. The developed unit enhances the technological capabilities of the process of plasma-arc atomization of current-carrying wires, as a specialized control system was developed for this purpose, which includes the measuring, starting and control and signal equipment, in particular, use of a touch panel, programmable logic controller (PLC) and development of the re-

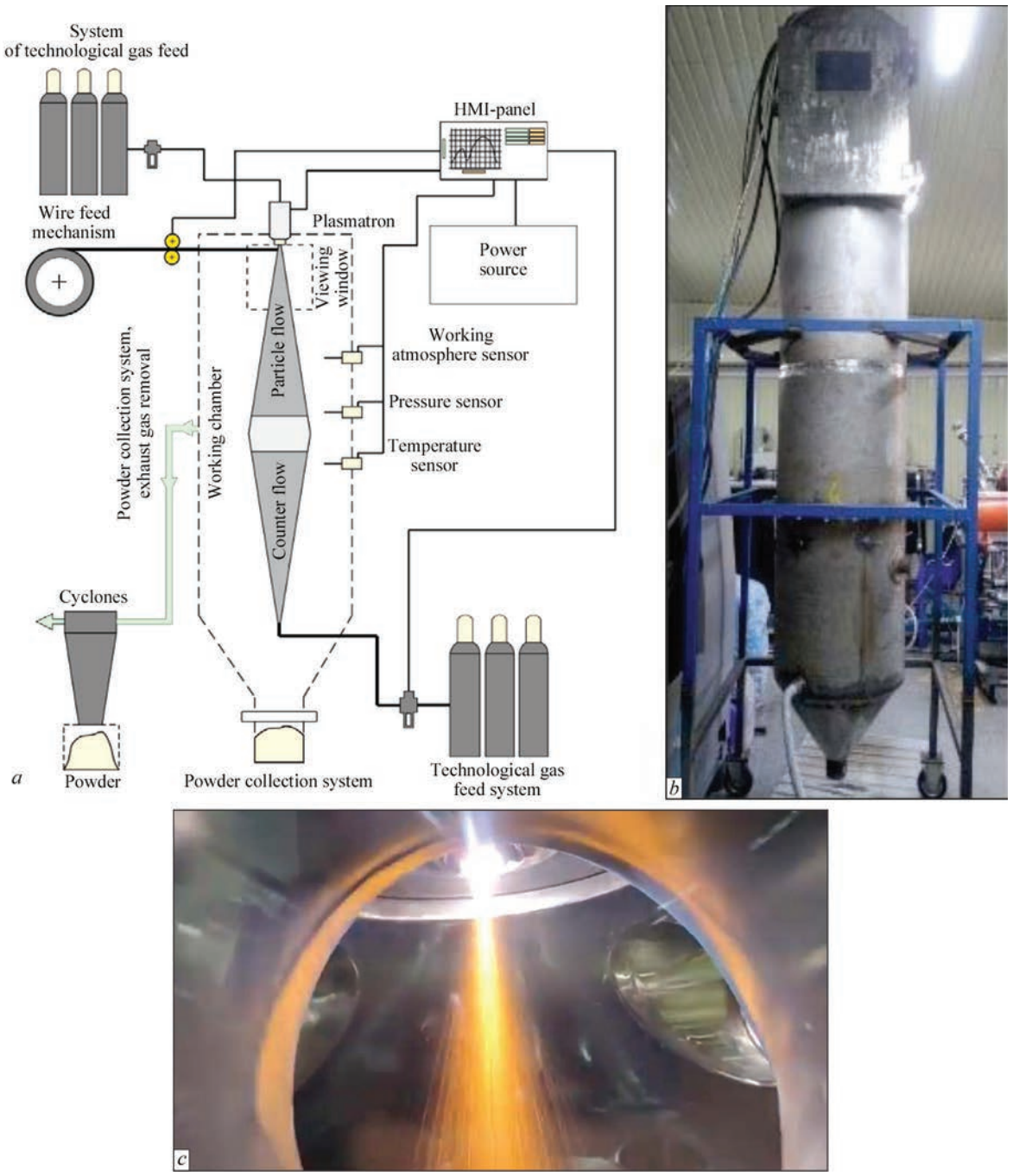

Figure 6. Scheme (*a*) and appearance (*b*) of experimental-production equipment and visualization (*c*) of the process of plasma-arc spheroidization of current-carrying materials with a chamber with protective atmosphere and counter gas flow

spective software. The unit software contains all the functions of control, adjustment, indication and emergency signaling of the unit operation modes. PLC has the function of an executive computing device, which on the basis of the data received from the monitoring system, performs correction of atomization process parameters and equipment operation algorithm, changing current, gas flow rates, wire feed rate, etc.

PWI developed an experimental-production unit for plasma-arc spheroidization of current-carrying materials (Figure 6), where a counter gas flow is used for control and monitoring of the speed and temperature characteristics of the granules. It allows greatly reducing the overall dimensions of the atomization chamber to 3 m chamber height, as the standard production chambers have not less than 10–15 m chamber height, and regulating the rate of particle cooling inside the chamber, in particular for formation of a fine-crystalline structure.

Numerical modeling means were used for calculation of the main structural parameters of this chamber, and for selection of optimal velocities of the counter gas flow. For this purpose, first modeling of the process of outflowing of argon plasma blown by an accompanying gas flow was performed in CFD software, by solving a system of MHD equations (5–12) and using a standard two-parametric *k–e* model of turbulence (13), and gas-dynamic and temperature characteristics of the plasma jet were defined (Figure 7):

1. Law of mass conservation:

$$\nabla \rho \upsilon. \tag{5}$$

2. Law of momentum conservation:

$$\rho\left(\vec{V}\cdot\nabla\vec{V}\right)=\vec{j}\cdot\vec{B}-\nabla p+\frac{2}{3}\mu\left(\nabla\vec{V}\right)+2\nabla\cdot\left(\mu\vec{S}\right). \tag{6}$$

3. Law of energy conservation:

$$\nabla\cdot\left(\rho\vec{V}h\right)=\nabla\cdot\left(\lambda\nabla T\right)+\vec{j}\cdot\vec{E}+\frac{5}{2}\frac{k_B}{e}\vec{j}\cdot\nabla T. \tag{7}$$

4. Maxwell equation:

$$\nabla\cdot\left(-\sigma\nabla\varnothing\right)=0, \tag{8}$$

$$\vec{E}=-\nabla\varnothing, \tag{9}$$

$$\nabla^2\vec{A}=-\mu_0\vec{j}, \tag{10}$$

$$\vec{B}=\nabla\cdot\vec{A}. \tag{11}$$

5. Ohm's law

$$\vec{j}=\sigma\cdot\vec{E}. \tag{12}$$

where ρ is the gas density, kg/m^3; $\vec{V}$ is the gas velocity, m/s; $\vec{j}\cdot\vec{B}$ is the Lorentz force due to electric current vector $\vec{j}$, A/m^2; and electromagnetic induction vector, $\vec{B}$, T; p is the pressure, Pa; μ is the dynamic viscosity of plasma, kg/m.s; $\vec{S}$ is the strain rate tensor; h is the enthalpy, J/kg; $\vec{E}$ is the electric field, V/m; k_B is the Boltzmann constant, J/K^{-1}; e is the elementary charge, C; σ is the electric conductivity of gas, W/m·K; Ø is the electrostatic potential, V; $\vec{A}$ is the vector potential of the electromagnetic field, T·m.

$$\mu_t=\rho C\frac{k^2}{\varepsilon}, \tag{13}$$

where k is the kinetic energy of turbulence, m^2/s^2; ε is the turbulent energy dissipation rate, m^2/s^3; ρ is the medium density, kg/m^3; C = 0.09; μ_t value has the dimension of kg/m·s.

At the next stage the Taylor Analogue Break-up (TAB) model of hydrodynamic break-up of the drops and the derived experimental data were used to model the process of dispersion of the melt forming during plasma-arc atomization at the edge of current-carrying 1.6 mm wire from AISI 316 steel (14–17). TAB model draws an analogy between the mass-spring-damper system and oscillations and deformation of the liquid drops leading to their refinement. In this analogy the surface tension force is represented by the restoring or stabiliz-

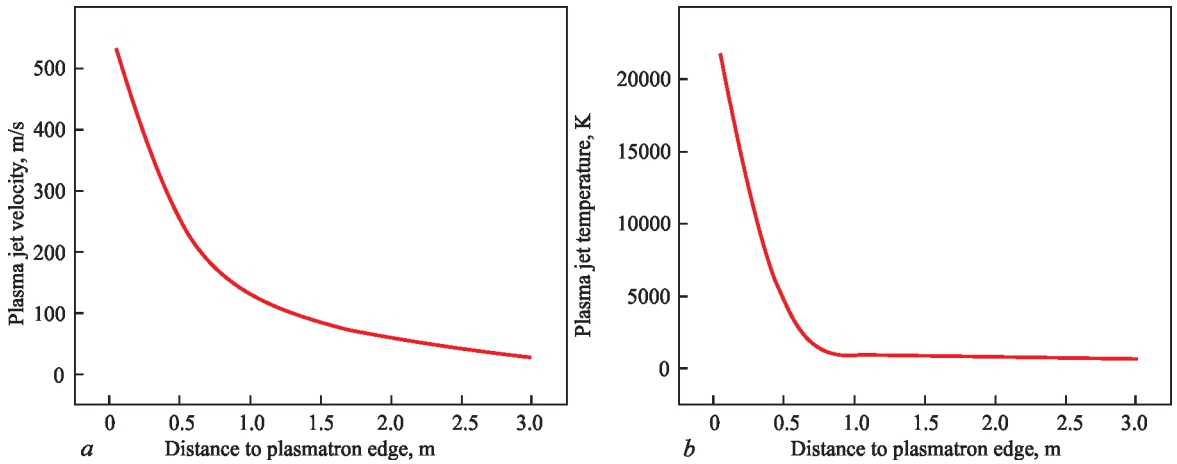

Figure 7. Gas-dynamic (*a*) and temperature characteristics (*b*) of argon plasma, blown by accompanying gas (P = 16 kW)

ing force of the spring, while the aerodynamic force of the gas is the source of external force, or the force, which destabilizes the mass, and the damping force is represented by the liquid viscosity characteristic:

$$m\ddot{x} = F - kx - d\dot{x}, \quad (14)$$

where m, F, k and d are the mass, force, spring constant and damping constant, respectively; x is the displacement of the drop equator from the equilibrium position in the form of a sphere to an oblate ellipsoid (Figure 8).

Using the Taylor's analogy coefficients, the physical dependencies of the coefficients in equation (14) have the following values:

$$\frac{F}{m} = C_f \frac{\rho_g u^2}{\rho_l r}, \quad (15)$$

$$\frac{k}{m} = C_k \frac{\sigma}{\rho_l r^3}, \quad (16)$$

$$\frac{d}{m} = C_d \frac{\mu_l}{\rho_l r^2}, \quad (17)$$

where ρ_l is the drop density, kg/m^3; ρ_g is the density of the continuous phase, kg/m^3; u is the relative speed of the drop, m/s; r is the initial drop radius, m; σ is the drop surface tension force, N/m; μ_l is the drop dynamic viscosity, kg/m·s. Values for dimensionless constants are as follows: $C_f = 0.33$; $C_d = 5$ and $C_k = 8$.

It was found that during atomization, particles the dimensions of which can be in the range of 20 to 500 μm, are formed. Investigations of these particles movement and their heat exchange with the atmosphere inside the atomization chamber (Figure 9) showed that at 3 m distance from the plasmatron edge their speed can be in the range of 8–30 m/s, depending on the calculated dimensions, and their temperature can be equal to 400–1200 K. This, in its turn, leads to particle deformation and formation of defective

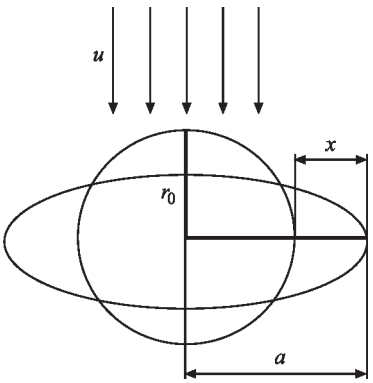

Figure 8. Drop deformation mechanism in keeping with TAB model

products at their collision with the walls of powder collector (at calculated chamber height, equal to 3 m).

It is shown that the counter gas flow allows performing processing in atomization chambers of not more than 3 m length, due to intensification of particle braking processes, and increasing the rate of heat exchange between the atmosphere and the particles (Figure 10).

Experimental studies of the sphericity coefficient of granules from AISI 316 stainless steel (Figure 11), produced at atomization in different atmospheres, showed that compared to atomization in air, use of chambers with a shielding argon atmosphere and counter gas flow allows increasing the sphericity coefficient of the granules from 0.73 to 0.85.

PWI is also performing studies of the processes of plasma-arc spheroidization of neutral (Figure 12, *a*) and current-carrying wires (Figure 12, *b*) and rods, using plasmatrons with a hollow copper anode, operating at reverse polarity.

It was found that the method of reverse polarity plasma-arc atomization (by the "wire–cathode" and neutral wire scheme) has a number of advantages among the currently available plasma spheroidization technologies, which are of wide practical interest, as:

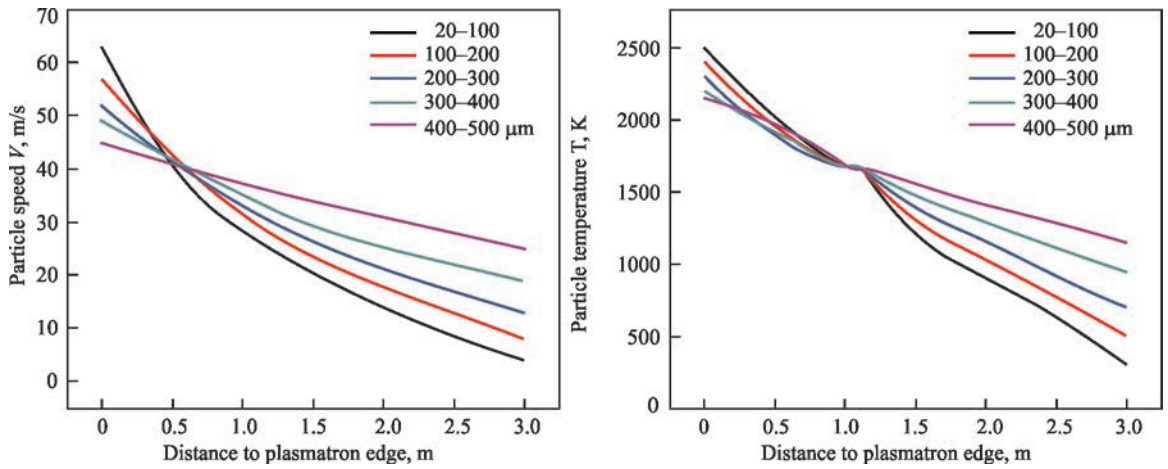

Figure 9. Dependence of the change in particle speed V (*a*) and temperature T (*b*) at a certain distance from plasmatron edge (without using counter gas flow)

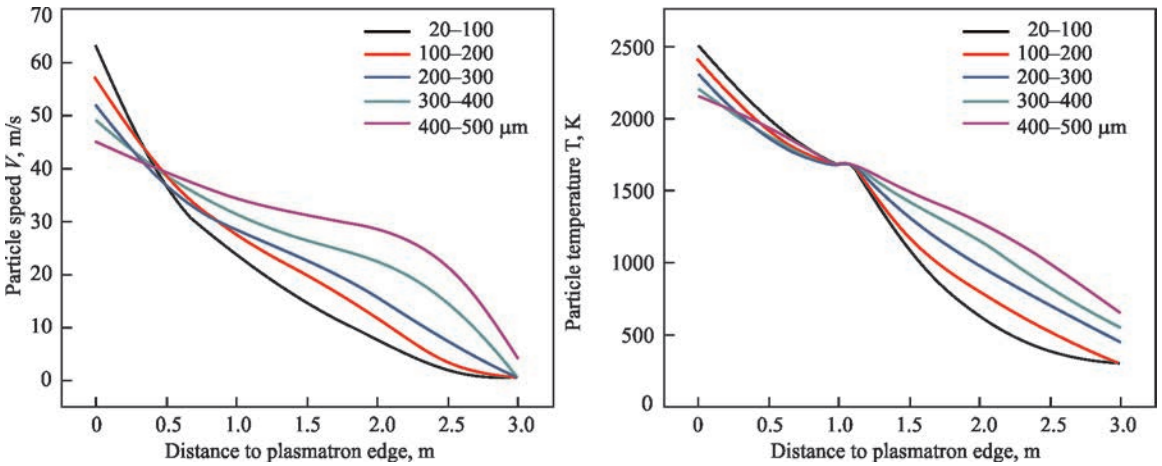

Figure 10. Dependence of the change in particle speed *V* (*a*) and temperature *T* (*b*) at a certain distance from plasmatron edge (using counter gas flow)

● they allow increasing electric power (up to 200 kW) due to "elongation" of the arc (from 150 to 550 V) in the copper electrode cavity owing to a change of the jet gas-dynamic characteristics, unlike plasmatrons operating at straight polarity, where increase of electric power is achieved by increasing the working current (from 400 to 1000 A), using high capacity power sources, which intensifies erosion of the nozzle and the electrode, or using plasmatrons of a more complex design (water-cooled IEI etc.)

● they enable dispersion of a wide range of sprayed materials (from large-diameter solid and flux-cored wires to rods of 50 mm and greater diameter, etc.);

● plasmatron design allows generation of a supersonic plasma jet with the velocity in the range of (1.5–4.0)·10^3 m/s, which greatly intensifies the processes of dispersion of the melt, forming at the spraying electrode edge, and increases the amount of the produced fine fraction (<80 μm) of the granules [26];

● a low rate of erosion (0.01 nanogram/C at 40 kW) of the electrode is achieved, which does not have any limitations as to the number of its operation starts, which also greatly prolongs the plasma equipment service life;

● thermal efficiency of plasmatrons with a hollow copper cathode is on the level of 0.80–0.85, here the power transferred to the product by the plasma flow, P_{pl} at the same operation modes is 1.2 to 1.5 times greater, than at straight polarity. It results in improvements of the process efficiency, allowing a significant reduction of the amount of energy consumed in melting one unit of the wire volume [27].

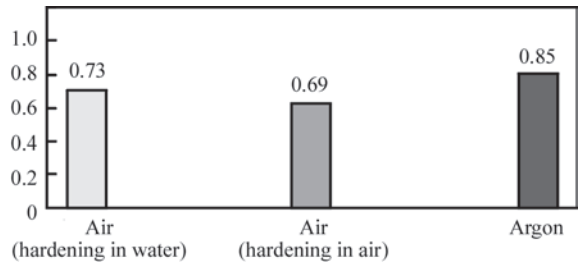

Figure 11. Dependence of sphericity parameters of sprayed particles from AISI 316 stainless steel of 20–100 μm fraction on ambient atmosphere type (*P* = 16 kW): *1* — air (hardening in water); *2* — air (hardening in air); *3* — argon

The data obtained at numerical modeling of the abovementioned process (Figure 13) confirmed that at plasmatron operation at reverse polarity current, arc voltage *U* is much higher than when working at straight polarity, $U_{RP} \approx (1.1–1.5)U_{SP}$ (U_{RP} is the constricted arc voltage at plasmatron operation at reverse polarity, U_{SP} is the constricted arc voltage during plasmatron operation at straight polarity), resulting in higher productivity of the plasmatron [28].

In accordance with that a line of plasmatrons were developed for atomization of neutral and current-car-

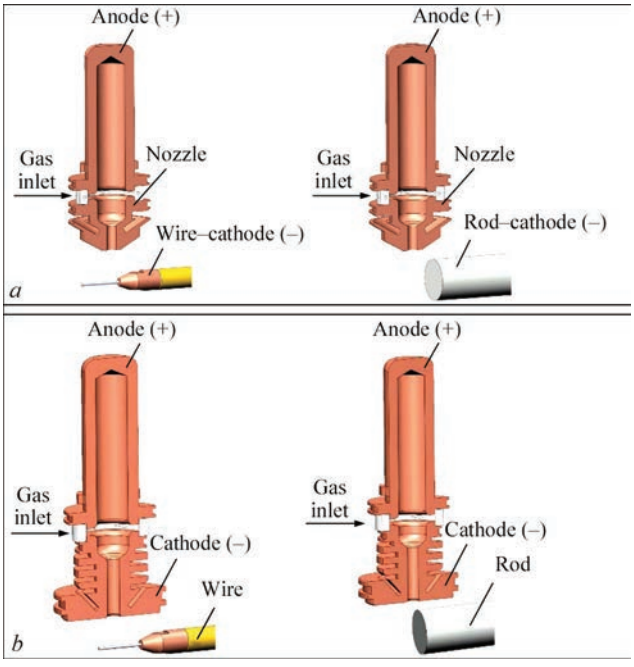

Figure 12. Scheme of plasma-arc atomization process at reverse polarity using plasmatrons with a copper hollow anode: current-carrying (*a*) and neutral (*b*)

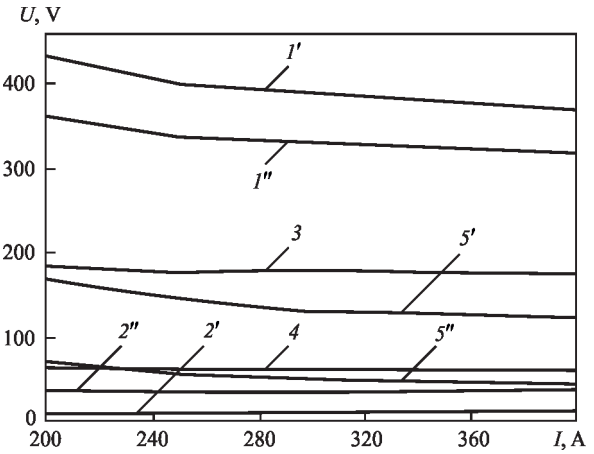

Figure 13. Dependence of constricted arc voltage on current: *1* — total arc voltage; *2* — voltage inside hollow electrode; *3* — voltage in the nozzle plasma-forming channel; *4* — voltage in open section of the arc; *5* — voltage in the cut cavity at plasmatron operation at reverse (*1′*, *5′*) and straight polarities (*1″*, *5″*)

rying materials, using approaches established when designing and manufacturing the plasmatrons for reverse polarity cutting.

PRODUCING SPHERICAL GRANULES BY PLASMA-ARC ATOMIZATION OF WIRE MATERIALS

Experiments on atomization of various types and grades of current-carrying compact (Figure 14, *a*) and flux-cored wires (Figure 14, *b*) were performed in PLAZER-50-PL-W unit with further analysis of the technological and structural features of the produced granules.

So, investigation of particle size distribution of granules (Figure 15) produced at atomization of current-carrying compact wire from AISI 316 stainless steel, showed that owing to a large number of regulated parameters the above equipment allows producing spherical granules in the size range of 15–315 μm. Here, in certain atomization modes it is possible to obtain a large amount of fine fraction. The main fraction is 15–100 μm, which makes up to 90 wt.%,

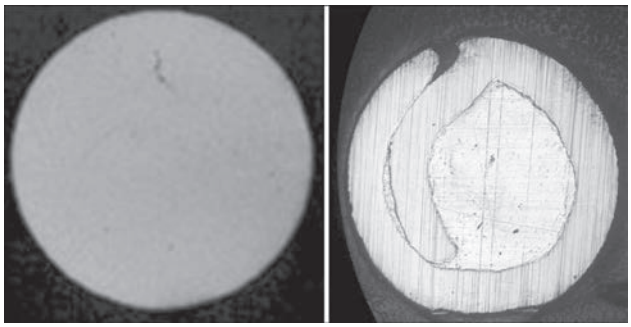

Figure 14. SEM images of the cross-section of compact wire from AISI 316 stainless steel (*a*) and flux-cored wire of Fe–Al(86Fe + 14Al wt.%) alloying system (*b*)

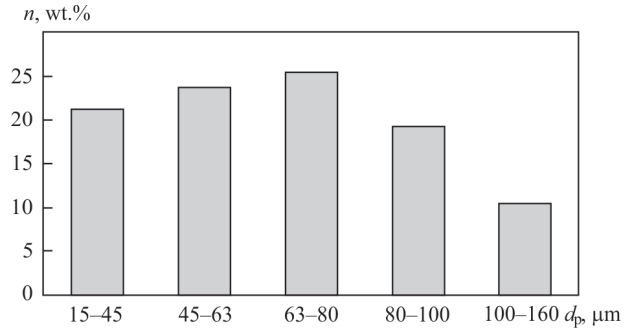

Figure 15. Particle size distribution of granules produced at atomization of compact wire from AISI 316 stainless steel

where the proportion of 15–45 μm fraction is equal to 21.2 wt.%, that of 45–63 μm fraction — 23.7 wt.%, that of 63–80 μm fraction — 25.4 wt.%, that of 80–100 μm fraction — 19.2 wt.%, that of 100–160 μm fraction — 10.5 wt.%, and the average diameter d_{50} = 63 μm.

Investigations of the shape of these granules showed that on the whole they are of a regular spherical shape (Figure 16, *a*) with sphericity coefficient S = 0.83 and higher, while the proportion of irregularly-shaped particles is not more than 1 wt.%.

Results of investigations of the technological properties of the abovementioned granules showed that their fluidity (in the case of –45; +15 μm frac-

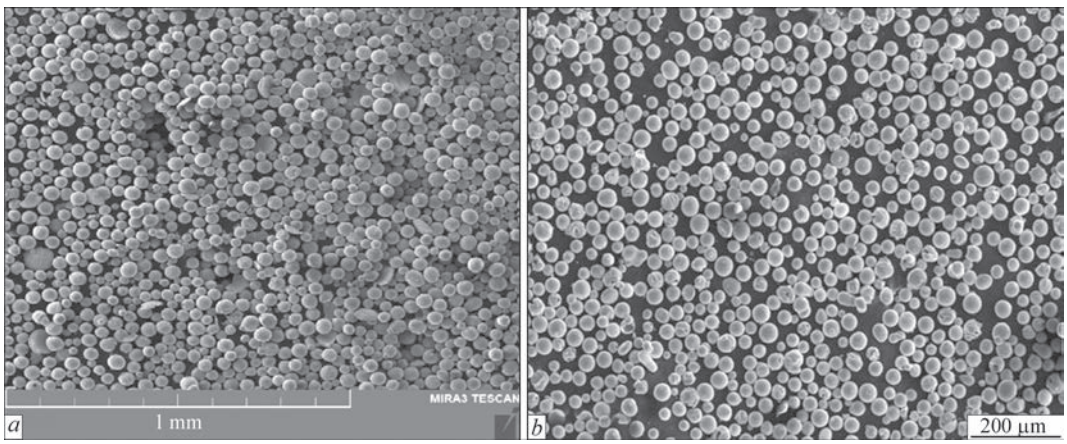

Figure 16. SEM image of granules produced at atomization of compact wire from AISI 316 stainless steel (*a*) and Ti Grade2 titanium (*2*) [31]

Table 2. Particle size distribution and fluidity of granules of different grades from 316 L stainless steel

Powder brand and production method	Fraction size, μm	d_{90}, μm	d_{50}, μm	d_{10}, μm	Fluidity, s/50 g
MetcoAdd 316-A, GA	–45; +15	46	30	19	<20
PLAZER-30, PA	–45; +15	43	28	17	18
GA [29]	–45;+15	45	22	8	29

Table 3. Particle size distribution of granules, produced at atomization of current-carrying compact wires of different chemical composition

Number	Material	Wire diameter, mm	Power, kW	Average granule diameter d_{50}, μm
1	Cu–ETP copper	1.2	21	52
2	AISI 316 stainless steel	1.0	18	63
3	NiCr-3 nickel alloy	2.0	21	184
4	Inconel 625 nickel alloy	1.2	22	87
5	Ti Grade 2 titanium	1.6	14	152

tion) is at the same level as that of another commercial powder of MetcoAdd 316-A grade (Oerlicon AM Co., Ltd, Germany), widely used by SLM and DMLS methods and it is equal to 18 s/50 g.

It should be also noted that the productivity of the abovementioned process for this mode of atomization of current-carrying wire from AISI 316 stainless steel (plasma arc power P = 18 kW and total argon flow rate Q = 25 m^3/h) is equal to 10.5 kg/h with further possibility of its increase. Table 3 gives the results of analysis of particle size distribution of granules produced at atomization of current-carrying compact wires of different chemical composition.

Investigations of the process of plasma-arc atomization of current-carrying flux-cored wire of Fe-Al alloying system, showed that the above process al-

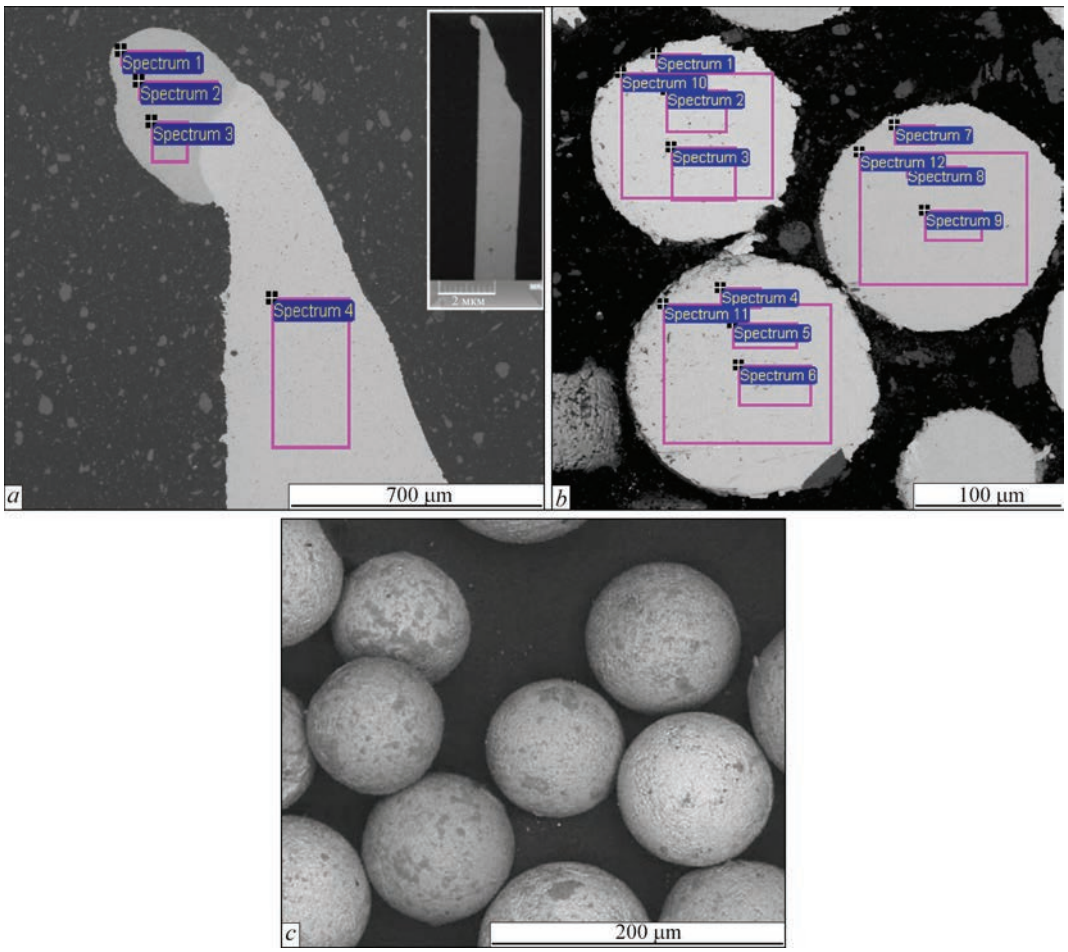

Figure 17. SEM image of Fe–Al wire edge after an abrupt extinguishing of the arc during plasma-arc atomization (*a*), granule microstructure (*b*) and appearance of particles (*c*): spectra 1–3 — zone of metallurgical interaction of the wire material at its melting and atomization; spectrum 4 — wire zone not subjected to thermal impact; spectra 1–12 — zone with granule cross-section

Table 4. Chemical composition of local zones at the edge of flux-cored wire–anode Fe–Al after an abrupt extinguishing of the arc during plasma-arc atomization and granule microstructure

Local zone number (spectrum)	Image	Chemical composition of local zones, at.%			
		Fe	Al	Si	O
1	Figure 17, *a*	76.49	23.51	–	–
2		75.49	24.51	–	–
3		74.15	25.85	–	–
4		99.64	–	0.36	–
1	Figure 17, *b*	82.92	16.04	0.55	0.49
2		82.67	16.31	0.70	0.32
3		83.01	16.44	0.21	0.34
4		74.07	25.09	0.63	0.21
5		74.78	24.62	0.46	0.14
6		74.44	24.94	0.43	0.19
7		71.67	27.71	0.20	0.42
8		72.52	27.52	0.00	0.23
9		71.59	28.01	0.13	0.27
10		83.17	16.22	0.24	0.37
11		74.10	25.03	0.71	0.16
12		71.75	27.85	0.12	0.28

lows producing spherical granules from high alloys (Figure 17, *c*), which are difficult or impossible to produce by the traditional methods (nickel, titanium, iron intermetallics and other alloys). Such granules further on can be used to manufacture products of a complex geometry, for instance by the technology of cold gas-dynamic spraying and further HT or TMT. The paper presents the results of experimental investigations of the processes of heating, melting and interaction of 86Fe + 14Al wt.% flux-cored wire, consisting of a steel sheath from St-08rim low-carbon steel and powder filler (aluminium of PA-4 grade) at optimal parameters of the atomization mode (18 kW power) in PLAZER-50-PL-W equipment. These studies showed that the above process allows producing spherical granules of a chemical composition, which practically does not differ from the composition of the initial material (flux-cored wire), while the proportion of granules with external and internal defects is not higher than 1.0–1.5 wt.% (Table 4) at average diameter d_{50} = 115 μm and up to 45 wt.% proportion of fine fraction of <100 μm.

Studies of melted-off edge of the flux-cored wire after an abrupt extinguishing of the arc, using X-Ray microspectral analysis (Tescan MIRA 3 LMU) showed that at the wire edge metallurgical interaction of the molten metal sheath and the aluminium filler takes place, leading to formation of a melt, the integral chemical composition of which corresponds to intermetallic of Fe_3Al type (Figure 7, *a*, Table 4). Investigation of the heterogeneity of intermetallic granules of different fractions (Table 4) showed a small inhomogeneity of chemical composition of the produced granules. So, Al proportion can vary from 16 to 28 at.%. At the same time, however, investigation of the granule phase composition by the method of X-Ray diffraction phase analysis (DRON-3M, CuK_α-radiation) showed that the proportion of Fe_3Al intermetallic phase can be up to 85 wt.%.

PRODUCING SPHERICAL GRANULES BY PLASMA-ARC ATOMIZATION OF RODS AND INGOTS

Experiments on atomization of current-carrying compact wire of 1.6 mm diameter from low-carbon steel of ER70S-6 grade and stationary rod of 50 mm diameter from low-carbon Q235 steel at 120 kW power of the plasma arc were performed in PLAZER-50-PL-W unit, upgraded for plasma atomization at reverse polarity.

Analysis of particle size distribution of granules (Figure 18) produced at atomization of current-carrying wire showed that during atomization spherical granules in the size range of 15–630 μm are

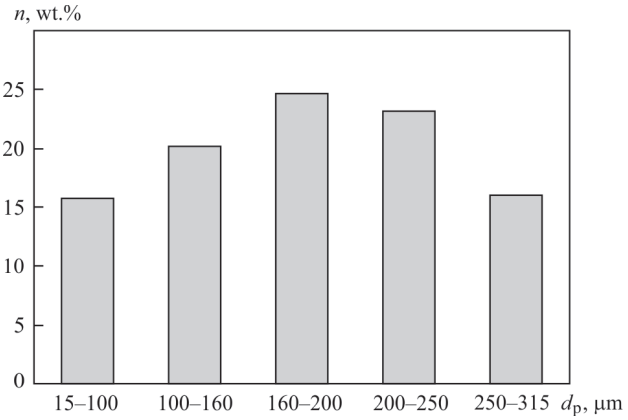

Figure 18. Particle size distribution of granules produced at atomization of current-carrying compact ER70S-6 wire of 1.6 mm diameter by plasmatron at reverse polarity and 120 kW power

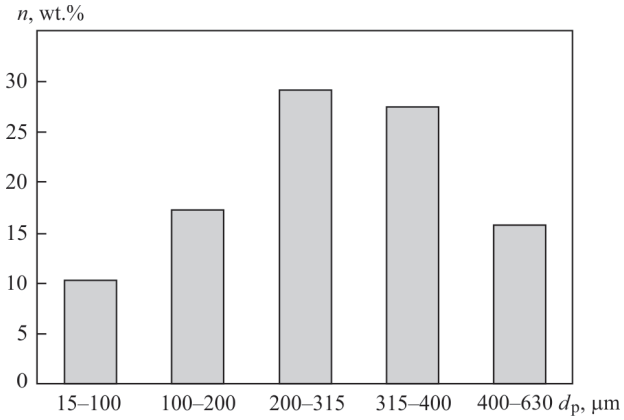

Figure 19. Particle size distribution of granules produced at atomization of a current-carrying stationary rod from low-carbon Q235 steel rod of 50 mm diameter by a plasmatron at reverse polarity and 120 kW power

formed, with the following percentage of fractions: 15–100 μm — 15.8 wt.%, 100–160 μm — 20.2 wt.%, 160–200 μm — 24.7wt.%, 200–250 μm — 23.2 wt.%, 250–315 μm — 16.1 wt.%, and the average diameter is d_{50} = 183 μm.

Analysis of particle size distribution of the granules (Figure 19), produced at atomization of current-carrying wire, showed that during atomization spherical granules in the size range of 15–630 μm are formed, with the following percentage of fractions: 15–100 μm — 10.3 wt.%; 100–200 μm — 17.2 at.%; 200–315 μm — 29.2 wt.%, 315–400 μm — 27.5 wt.%, 400–630 — 15.8 wt.%, average diameter being equal to d_{50} = 282 μm.

Study of the produced granules shape (Figure 20) showed that on the whole they have a regular spherical shape (Figure 20, *a*) with sphericity coefficient S = 0.75 and more, and the proportion of irregularly-shaped particles is not more than 5 wt.%. The productivity of atomization process at 120 kW power can be up to 16 kg/h for current-carrying compact wire from low-carbon ER70S-6 steel of 1.6 mm diameter, and in the case of atomization of a stationary rod from low-carbon Q235 steel of 50 mm diameter it is 20 kg/h. Here, a tendency is also observed to further improvement of productivity at increase of plasma arc power to 200 kW.

Thus, despite a high productivity the above process requires further investigations and development of additional technological measures, which will allow a significant increase of the amount of the fraction, suitable for application in AM and granule metallurgy technologies.

CONCLUSIONS

1. Critical analysis of modern technologies for producing spherical granules showed that in the general case the technologies of gas atomization are characterized by the presence of a large number of satellites and irregularly-shaped particles, lower coefficient of sphericity and intragranular argon-induced porosity, leading to formation of defects in the deposited layers and causing a significant lowering of the values of ultimate strength, impact toughness and other mechanical characteristics of finished products. The Plasma Rotating Electrode Process allows avoiding the majority of these disadvantages. Equipment operation, however, involves considerable difficulties for producing a fine fraction of <100 μm. To achieve more than 50 wt.% yield of the mentioned fraction, there is the need for an essential increase of the billet rotation speed (more than 30000 rpm), which greatly complicates the already not at all simple kinematic diagram of the unit (lowering of the level of vibrations, designing complex bearing systems, etc.). There are also difficulties associated with producing the cylindrical billet of precise dimensions, which has to be polished with a high accuracy, etc.

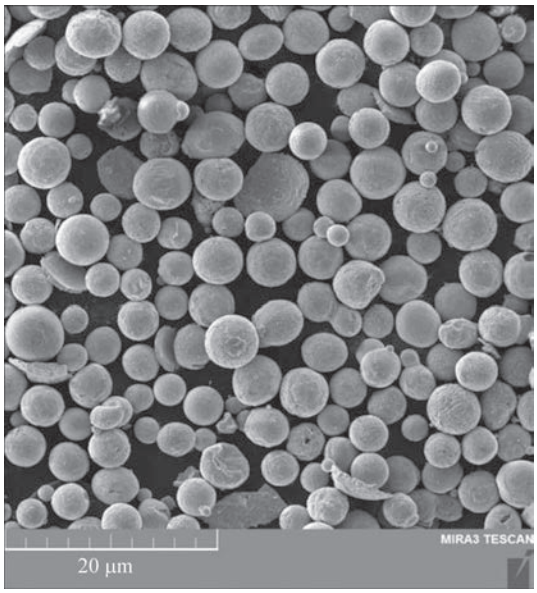

Figure 20. SEM images of granules produced at atomization in air of a current-carrying stationary rod from low-carbon Q235 steel of 50 mm diameter

2. It was found that the technology of plasma-arc atomization has considerable potential for further development and practical application in spherical granule manufacturing. One of its variants is the process of plasma-arc atomization of current-carrying and neutral wires, rods and large-sized ingots of up to 50 mm and greater diameter. The abovementioned process is characterized by higher values of energy efficiency and productivity, which can reach up to 20 kg/h, and relative simplicity of the equipment, and it allows producing spherical granules in a broad range of dimensions of 15–315 μm. Here, the amount of <100 μm fraction may reach 90 wt.%. A new generation PLAZER-50-PL-W unit was developed for

plasma-arc spheroidization of neutral and current-carrying wires and rods. Its feature is application of a plasmatron with higher current load and intelligent system of automatic real-time control and monitoring of a greater number of technological parameters. The designed atomization chamber with shielding atmosphere with gas counter flow allows a significant reduction of overall dimensions of the equipment, namely chamber height from 10–15 to 3 m, enables controlling particle cooling processes to form a finely-dispersed structure, and promotes producing spherical granules in the size range of 20–315 μm with the sphericity coefficient of 0.75–0.85.

3. Plasma-arc technologies developed at PWI allow producing spherical granules from the entire range of materials, widely used in the area of 3D printing of high-quality products by the methods of selective and direct laser melting and sintering, electron beam melting, cold gas-dynamic spraying and granule metallurgy technologies for producing high-quality structural metallic materials by compacting particles (granules) of a microcrystalline structure, which crystallized from the melt at a high rate.

REFERENCES

1. Iliyushchenko, A.F., Savich, V.V. (2017) History and state-of-the-art of additive technologies in Belarus, powders of metals and alloys for them. *Kosmichna Nauka i Tekhnologiya*, 23(**4**), 33–45 [in Russian]. DOI: https://doi.org/10.15407/knit2017.04. 033
2. Singh, D.D., Mahender, T., Reddy, A.R. (2021) Powder bed fusion process: A brief review. *Materials Today: Proceedings*, 46(**1**), 350–355. DOI: https://doi.org/10.1016/j.matpr.2020.08.415
3. Ahn, D.G. (2021) Directed energy deposition (DED) process: State of the art. *Int. J. of Precis. Eng. and Manuf. — Green Tech.*, **8**, 703–742. DOI: https://doi.org/10.1007/s40684-020-00302-7
4. Anderson, I.E. et al. (2018) Feedstock powder processing research needs for additive manufacturing development. *Curr. Opin. Solid State Mater. Sci*., 22(**1**), 8–15. DOI: https://doi.org/10.1016/j.cossms.2018.01.002
5. Chen, G., Zhao, S.Y., Tan, P. et al. (2018) A comparative study of Ti–6Al–4V powders for additive manufacturing by gas atomization, plasma rotating electrode process and plasma atomization. *Powder Technology*, **333**, 38–46. DOI: https://doi.org/10.1016/j.powtec.2018.04.013
6. Sun, P., Fang, Z., Zhang, Y. et al. (2017) Review of the methods for the production of spherical Ti and Ti alloy powder. *JOM*, **69**, 1853–1860. DOI: https://doi.org/10.1007/s11837017-2513-5
7. Heidloff, A.J., Rieken, J.R., Anderson, I.E. et al. (2010) Advanced gas atomization processing for Ti and Ti alloy powder manufacturing. *JOM*, **62**, 35–41. DOI: https://doi.org/10.1007/s11837-010-0075-x
8. Guo, K., Liu, C., Chen, S. et al. (2020) High pressure EIGA preparation and 3D printing capability of Ti–6Al–4V powder. *Transact. of Nonferrous Metals Society of China*, 30(**1**), 147–159. DOI: https://doi.org/10.1016/S1003-6326(19)65187-3
9. Martín, A., Cepeda-Jiménez, C.M., Pérez-Prado, M.T. (2020) Gas atomization of γ-TiAl alloy powder for additive manufacturing. *Adv. Eng. Mater.*, **22**, 1900594. DOI: https://doi.org/10.1002/adem.201900594
10. Drawin, S., Deborde, A., Thomas, M. et al. (2020) Atomization of Ti-64 alloy using the EIGA process: comparison of the characteristics of powders produced in labscale and industrial-scale facilities. *MATEC Web Conf.*, **321**, 07013. DOI: https://doi.org/10.1051/matecconf/202032107013
11. Zhong, C., Chen, J., Linnenbrink, S. et al. (2016) A comparative study of Inconel 718 formed by high deposition rate laser metal deposition with GA powder and PREP powder. *Materials & Design*, **107**, 386–392. DOI: https://doi.org/10.1016/j.matdes.2016.06.037
12. Zhao, Y., Cui, Y., Numata, H. et al. (2020) Centrifugal granulation behavior in metallic powder fabrication by plasma rotating electrode process. *Sci. Rep.*, 10, 18446. DOI: https://doi.org/10.1038/s41598-020-75503-w
13. *Yang* Liu, Xiao-hao Zhao, Yun-jin Lai et al. (2020) A brief introduction to the selective laser melting of Ti6Al4V powders by supreme-speed plasma rotating electrode process. Progress in Natural Science. *Materials Inter.*, 30(**1**), 94–99. DOI: https://doi.org/10.1016/j.pnsc.2019.12.004
14. Strogonov, D.V., Korzhyk,V.M., Jianglong Ti, et al. (2022) Influence of the parameters of the process of plasma-arc spheroidization of current-conducting wire from low-carbon steel on the granulometric composition of the produced powders. *Suchasna Elektrometal.*, **3**, 29–38 [in Ukrainian]. DOI: https://doi.org/10.1037434/sem2022.03.05
15. Yurtkuran, E., Ünal, R. (2022) Theoretical and experimental investigation of Ti alloy powder production using low-power plasma torches. *Transact. of Nonferrous Metals Society of China*, 32(**1**), 175–191. DOI: https://doi.org/10.1016/S1003-6326(21)65786-2
16. Tsantrizos, P.G, Allaire, F., Entezarian, M. (1998) *Method of production of metal and ceramic powders by plasma atomization*. US patent, 5707419 [P], 1998−01−13.
17. Cacace, S., Boccadoro, M., Semeraro, Q. (2023) *Investigation on the effect of the gas-to-metal ratio on powder properties and PBF-LB/M processability*. Prog. Addit. Manuf. DOI: https://doi.org/10.1007/s40964-023-00490-z
18. Korzhyk, V.M., Strogonov, D.V., Burlachenko, O.M. et al. (2023) New generation unit for plasma-arc deposition of coatings and spraying of current-conducting wire materials. *Suchasna Elektrometal.*, **3**, 19–27 [in Ukrainian]. DOI: https://doi.org/10.37434/sem2020.03
19. Korzhyk, V.M., Strogonov, D.V., Burlachenko, O.M. et al. (2023) Effectiveness of the process of plasma-arc spheroidization of current-conducting titanium wire. *Suchasna Elektrometal.*, **1**, 1–9 [in Ukrainian]. DOI: https://doi.org/10.37434/sem2023.01.05
20. Capus, J. (2017) AP&C: moving fast with the rise of AM. *Metal Powder Report*, 72(**1**), 22–24. DOI: https://doi.org/10.1016/j.mprp.2016.12.001
21. Petrunichev, V.A., Kudinov, V.V., Kulagin, I.D. (1965) Production of spheroidized metal powder by wire spraying. *Metally*, **2**, 68–94 [in Russian].
22. Zelenin, V.I., Kavunenko, P.M., Tisenkov, V.V. et al. (2009) Application of plasma-arc metallization for restoration of wheel pairs. *The Paton Welding J.*, **12**, 28–31.
23. Korzhik, V.N., Korob,M.F. (2012) Mechanized line PLAZER 30PL-W for plasma-arc wire spraying of coatings on large-sized parts of "shaft" type. *Svarshchik*, **4**, 13–15 [in Russian].
24. Kharlamov, M.Yu., Krivtsun, I.V., Korzhik, V.N. et al. (2008) Effect of the type of concurrent gas flow on characteristics of the arc plasma generated by plasmatron with anode wire. *The Paton Welding J.*, **6**, 14–18.
25. Kharlamov, M., Krivtsun, I., Korzhyk, V., Demyanov, O. (2015) Simulation of motion, heating and breakup of molten metal droplets in the plasma jet at plasma-arc spraying. *J. of Thermal Spray Technology*, **24**, 659–670. DOI: https://doi.org/10.1007/s11666-015-0216-4

26. Liu, F., Yu, D., Zhang, Q. et al. (2023) Experimental and numerical analysis of a novel reverse-polarity plasma torch with transferred arc hot-wall nozzle for atmospheric plasma spraying of YSZ coatings. *Surface and Coatings Technology*, **459**, 129413. DOI: https://doi.org/10.1016/j.surfcoat.2023.129413
27. Shchitsyn, V.Yu., Yazovskikh, V.M. (2009) Effect of polarity on the heat input into the nozzle of a plasma torch, *Welding International*, 16(**6**), 485–487. DOI: https://doi.org/10.1080/09507110209549563
28. Kharlamov, M.Yu., Krivtsun, I.V., Korzhik, V.N. et al. (2015) Modelling the characteristics of constricted-arc plasma in straight and reverse polarity air-plasma cutting. *The Paton Welding J.*, **10**, 10–18.
29. Bouabbou, A., Vaudreuil, S. (2023) Numerical modelling of SS316L powder flowability for laser powderbed fusion. *Archives of Materials Sci. and Engineering*, 120(**1**), 22–29. DOI: https://doi.org/10.5604/01.3001.0053.6014

ORCID
V.M. Korzhyk: 0000-0001-9106-8593,
D.V. Strohonov: 0000-0003-4194-764X,
O.M. Burlachenko: 0000-0003-2277-4202,
O.M. Voitenko: 0000-0003-4946-6517

CONFLICT OF INTEREST
The Authors declare no conflict of interest

CORRESPONDING AUTHOR
V.M. Korzhyk
E.O. Paton Electric Welding Institute of the NASU
11 Kazymyr Malevych Str., 03150, Kyiv, Ukraine
E-mail: vnkorzhyk@gmail.com

SUGGESTED CITATION
V.M. Korzhyk, D.V. Strohonov, O.M. Burlachenko, O.M. Voitenko, D.V. Kunitskyi (2023) Development of plasma-arc technologies of spherical granule production for additive manufacturing and granule metallurgy. *The Paton Welding J.*, **12**, 3–18.

JOURNAL HOME PAGE
https://patonpublishinghouse.com/eng/journals/tpwj

Received: 19.10.2023
Accepted: 26.12.2023